Journal of Healthcare Informatics Research (2025) 9:174–190
https://doi.org/10.1007/s41666-025-00192-x

RESEARCH ARTICLE

Dynamic Prediction and Intervention of Serum Sodium in Patients with Stroke Based on Attention Mechanism Model

Xiao Lu[1] · Hongli Xu[1] · Wei Dong[1] · Yi Xin[2] · Jiang Zhu[2] · Xingkang Lin[2] · Yan Zhuang[1] · Hebin Che[1] · Qin Li[2] · Kunlun He[1]

Received: 25 January 2024 / Revised: 14 February 2025 / Accepted: 17 February 2025 /
Published online: 6 March 2025

Abstract

Abnormal serum sodium levels are a common and severe complication in stroke patients, significantly increasing mortality risk and prolonging ICU stays. Accurate real-time prediction of serum sodium fluctuations is crucial for optimizing clinical interventions. However, existing predictive models face limitations in handling complex dynamic features and long time series data, making them less effective in guiding individualized treatment. To address this challenge, this study developed a deep learning model based on a multi-head attention mechanism to enable real-time prediction of serum sodium concentrations and provide personalized intervention recommendations for ICU stroke patients. This study utilized publicly available MIMIC-III ($n = 2346$) and MIMIC-IV ($n = 896$) datasets, extracting time series data from 10 key clinical indicators closely associated with serum sodium levels. To address the complexity of long time series data, a moving sliding window subsampling segmentation method was employed, effectively transforming extensive sequences into more manageable inputs while preserving critical temporal dependencies. By leveraging advanced mathematical modeling, meaningful insights were extracted from sparse and irregular time series data. The resulting time-feature fusion multi-head attention (TFF-MHA) model underwent rigorous validation using public datasets and demonstrated superior performance in predicting both serum sodium values and corresponding intervention measures compared to existing models. This study contributes to the field of healthcare informatics by introducing an innovative, data-driven approach for dynamic serum sodium prediction and intervention recommendation, providing a valuable clinical decision-support tool for optimizing sodium management strategies in critically ill stroke patients.

Xiao Lu and Hongli Xu are co-first authors and contributed equally to this paper.

Extended author information available on the last page of the article

Keywords ICU · Irregular sampling · Stroke · Serum sodium · Dynamic prediction model

1 Introduction

Abnormal serum sodium levels are a prevalent electrolyte imbalance in intensive care units (ICUs) and a common complication of acute severe stroke. This condition is intricately linked with increased mortality rates and extended ICU stays, presenting a significant clinical challenge [1]. Particularly in stroke treatment involving elevated intracranial pressure (ICP), the fluctuation of serum sodium levels is a critical factor influencing patient outcomes [2, 3]. Despite its significance, current clinical practices in managing serum sodium rely heavily on manual, subjective evaluations by physicians, leading to inconsistencies in decision-making. Given the World Health Organization's data that ranks stroke as the second leading cause of death globally [4] and the rising incidence and high mortality rate of stroke in China [5], the necessity for refined management of severe stroke patients is undeniable.

Recent studies highlight that abnormal serum sodium levels are observed in 12.2–17.1% of stroke patients [6–8]. Specifically, a study of 1268 stroke patients revealed a higher prevalence of abnormal serum sodium in severe cases compared to mild ones [6]. Further research emphasizes the correlation between in-hospital mortality and complications like abnormal serum sodium and upper gastrointestinal hemorrhage, particularly in primary intracerebral hemorrhage cases [6]. Epidemiological studies indicate varying mortality rates associated with hyponatremia, depending on the underlying diseases [9–12]. The exact etiological mechanisms linking abnormal serum sodium to mortality remain elusive, with hypotheses ranging from oxidative stress caused by hyponatremia [13] to activation of the vasopressor system.

Current clinical guidelines for severe stroke treatment recommend hypertonic saline (HTS) to manage increased ICP [2, 3]. However, the literature presents conflicting views regarding the association between HTS-induced hypernatremia and patient mortality [14, 15]. These contrasting findings underscore the need for further investigation into the prognostic implications of HTS treatment and the development of safe treatment strategies.

The complexity of severe patient conditions in ICUs necessitates real-time clinical decision-making tools. Hospital electronic health records (EHR) have amassed vast amounts of clinical data, including substantial objective data generated in ICUs during diagnosis and treatment processes [16]. However, the inherent irregularity in hospital visits and the variability in physiological variables examined during each visit result in large volumes of irregular multivariate time series data (IMTS), often with missing values and varying intervals, as illustrated in Fig. 1 [17, 18]. With the development of artificial intelligence, deep learning and time series models have been studied and applied in the field of clinical medicine. Recent studies include anomaly detection in multivariate time series data using deep ensemble models [19], rapid deep learning-assisted predictive diagnostics for point-of-care testing [20], and cardiac arrhythmia classification using advanced deep learning techniques

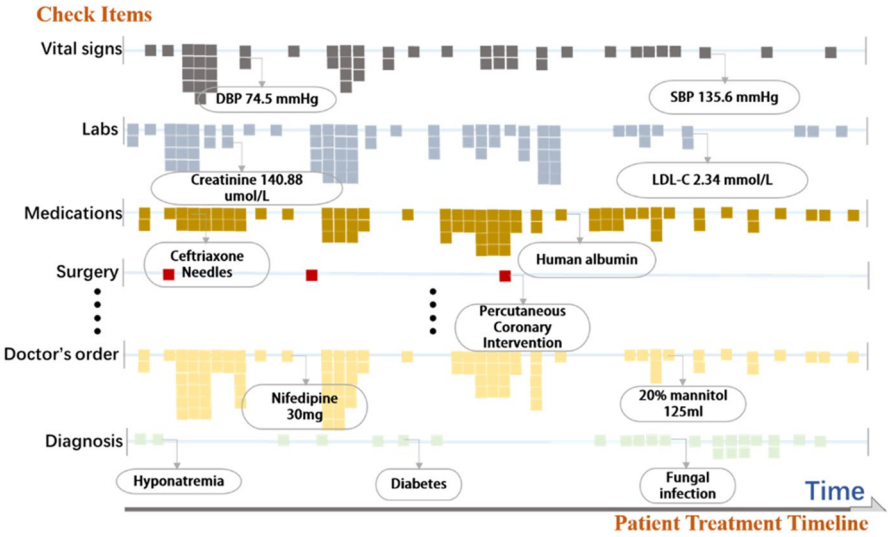

Fig. 1 Schematic diagram of irregular multivariable time series in real-world electronic medical record data. The horizontal axis represents the timeline of the patient's hospitalization, while the vertical axis reflects various categories of hospitalization information recorded at different time points. These include laboratory test indicators, medication details, doctor's orders, and diagnoses. Different colored boxes are used to distinguish between these categories, visually representing the diverse types of information recorded during the hospitalization period

on digitized ECG datasets [21]. These studies highlight the significant potential of deep learning in disease detection, diagnostics, and clinical decision support. Traditional methods that process IMTS into regular data for standard machine learning applications often fall short due to their inability to handle irregular time intervals effectively [22–26]. The natural and common occurrence of irregular sampling in EHRs, driven by patient status and symptom changes, underscores the importance of developing a model capable of handling these irregularities. In clinical practice, the capacity to accurately forecast serum sodium dysregulation and delineate appropriate intervention strategies in advance is critically significant. This proactive approach is instrumental in circumventing detrimental consequences that arise from tardiness in the implementation of clinical measures.

2 Methods

2.1 Data Sources and Patients

This research, aligned with ethical standards, received approval from the ethics committee of the PLA General Hospital. It was conducted in adherence to the World Medical Association Declaration of Helsinki Ethical Principles for Medical Research Involving Human Subjects. We sourced our data from the Medical Information Mart for Intensive Care (MIMIC) open-source clinical databases: MIMIC-IV

[27] and MIMIC-III [28]. Authorized access to these databases was granted, and all reports were prepared following the Strengthening the Reporting of Observational Studies in Epidemiology (STROBE) guidelines [29].

Patients with stroke were identified in the MIMIC-IV dataset using ICD10 codes I60, I61, and I63 and in the MIMIC-III dataset using ICD9 codes 4340, 43,401, 43,410, 43,411, 43,490, 43,491, 4370, 4373, and 4374. We excluded patients under 18 years of age and those with completely missing measurement indicators. As illustrated in Fig. 2, the data extraction and processing flowchart included 2346 and 896 stroke patients from MIMIC-III and MIMIC-IV, respectively. We meticulously extracted time series records of 10 features closely associated with current serum sodium concentration. For the purpose of training our time-feature fusion attention model (TFF-AM), we generated a comprehensive dataset: 31,428 training samples from MIMIC-IV, 11,547 internal validation samples from MIMIC-IV, and 28,618 testing samples from MIMIC-III. This dataset was derived through time window segmentation, using a 48-h window as a standard measure. Following fivefold cross-validation, the model was trained to output three distinct prediction results: the detection of abnormal blood sodium, the precise value of blood sodium, and the intervention measures required for managing blood sodium levels.

2.2 Data Extraction and Processing

Our approach to data extraction and processing focused on rigorously analyzing the time series records of 10 key features that are closely associated with the serum sodium concentration in stroke patients during their hospitalization. These critical features encompass serum potassium, serum chlorine, previous serum sodium, glucose, serum magnesium, urea, serum calcium, bicarbonate, sodium-water volume, and liquid in–out. The selected ten time series indicators are key clinical

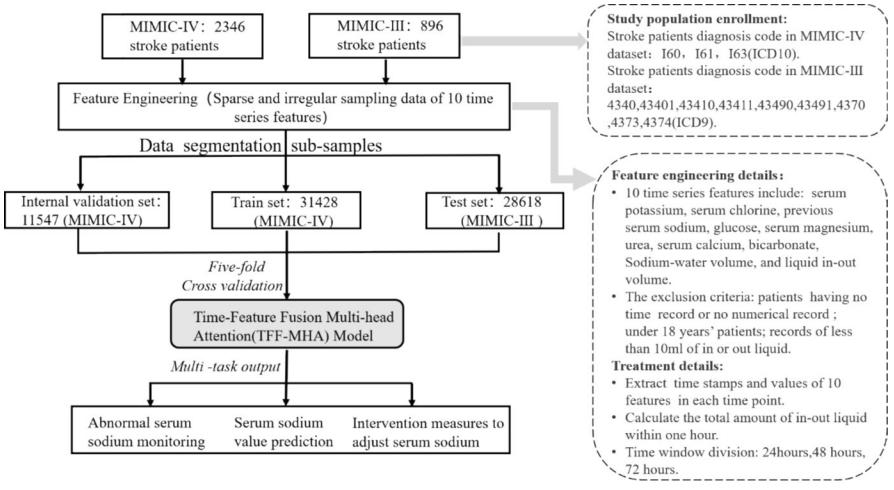

Fig. 2 Data extraction and processing flowchart

parameters closely associated with electrolyte balance, metabolic function, and fluid status, making them crucial for predicting serum sodium and potassium levels and informing intervention strategies. Specifically, serum potassium, chlorine, calcium, and magnesium reflect the core status of electrolyte dynamics, while previous serum sodium provides historical trends of the patient's condition. Glucose and urea are highly correlated with electrolyte metabolism and kidney function. Bicarbonate directly represents acid–base balance, and sodium-water volume along with fluid in–out reflects the dynamic regulation of body fluids and sodium metabolism. By integrating these indicators, the model effectively captures complex pathophysiological variations, significantly enhancing the accuracy of serum sodium and potassium predictions and the scientific basis for intervention strategies. Initially, we extracted the pertinent data from the raw MIMIC-III and MIMIC-IV datasets, meticulously organizing it by each patient's record. In the first phase of data filtering, we excluded all ICU records for patients under the age of 18. This exclusion was based on the substantial physiological differences between pediatric and adult patients, which could significantly impact the study's outcomes. Furthermore, we eliminated records of patients with incomplete data, specifically those lacking either time stamps or numerical values in their records, to ensure data integrity. Moving to the next phase, as illustrated in Fig. 3, we identified the current time point with recorded serum sodium levels, denoted as time point "t." From this reference point, we extracted three distinct datasets representing the complete time series of the 10

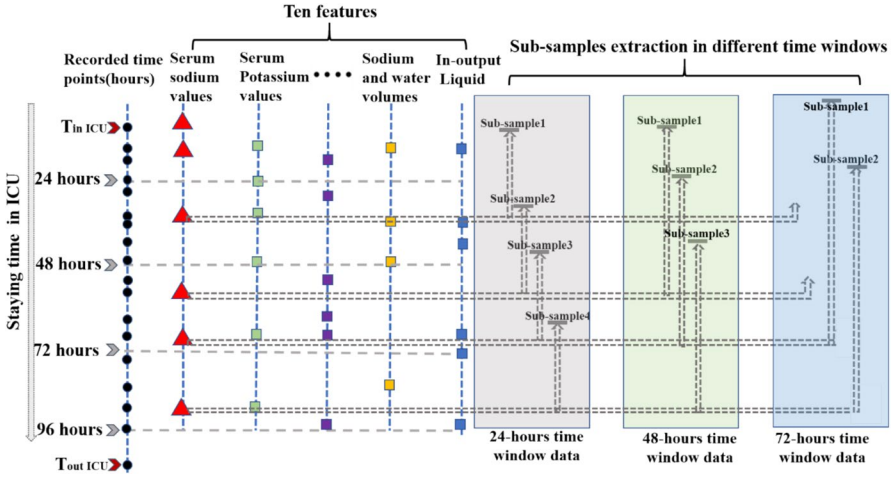

Fig. 3 Schematic diagram of subsample segmentation in different time windows. The black dots represent the time points recorded for each detection indicator, while different colored shapes represent the values of various indicators at different time points. For example, red triangles denote the time points corresponding to blood sodium measurements, while green squares represent blood potassium. In total, 10 time series indicators are recorded (in the figure, the other seven indicators have been omitted). The time window segmentation starts from the time point when the blood sodium value (represented by the red triangle) appears and pushes backward by 24 h, 48 h, and 72 h, respectively, to collect data for these 10 indicators to establish different sub-datasets. The long gray box represents the subsample of the 24-h time window, the long green box represents the subsample of the 48-h time window, and the long blue box represents the subsample of the 72-h time window

indicators. These datasets covered the periods of 24 h, 48 h, and 72 h preceding time point "t." This methodological approach allowed for a comprehensive temporal analysis of the indicators. Additionally, we adopted specialized techniques to extract accurate information regarding sodium and water in-output volume, which included data on feeding, water injections through a gas tube, and inward injections. This thorough and systematic processing of data was essential to ensure the reliability and accuracy of our study's findings.

Next, we will extract information from three groups of subsamples from multiple perspectives. Firstly, we introduced the notations for multivariate time series data and then described our proposed method that consists of (i) input and time embedding and (ii) time-feature fusion learning. Before data subsample segmentation, for each subject n, given a set of D-dimensional multivariate time series in $\tau^{(n)}=[\tau_1, \ldots,\tau_i, \ldots,\tau_{Tn}]$ time points of length Tn, we denote an observation time series as $D^n = \left[D^n_{\tau 1}, \cdots, D^n_{\tau i} \cdots, D^n_{\tau Tn}\right]^T \epsilon R^{T_n} \times D$, where $D^n_{\tau i} \in R^D$ represents the τ_i-th observation of all variables, and $D^n_{\tau i,\theta}$ is the element of the θ-th variable in$D^n_{\tau i}$. In this setting, since the time series $D(n)$ includes missing values, we introduce the masking vector across time series, $M^n = \left[m^n_{\tau 1}, \cdots, m^n_{\tau i} \cdots, m^n_{\tau Tn}\right]^T \epsilon R^{Tn \times D}$, which has the same size of $D(n)$ to mark which variables are observed or missing. Specifically, we have $m^n_{\tau i,\theta} = 1$ if $D^n_{\tau i,\theta}$ is observed, otherwise,$m^n_{\tau i,\theta} = 0$. If the observation is missing, the input is set to zero for that dimension. For each variableθ, we also present the time interval $\Delta^n = \left[\varphi^n_{\tau 1}, \cdots, \varphi^n_{\tau i} \cdots, \varphi^n_{\tau Tn}\right]^T \epsilon R^{T_n \times D}$, where $\varphi^{(n)}_{\tau_i,\theta}$ is defined as formula (1). In our research, we are given a clinical time series dataset $\omega = \{(\boldsymbol{D}^n, \boldsymbol{M}^n, \Delta^n)\}_{n=1}^N$ for N subjects; we construct a function to predict the value of serum sodium of the stroke patients in ICU.

$$\varphi^{(n)}_{\tau_i,\theta} = \begin{cases} \tau_i - \tau_{i-1} + \varphi^{(n)}_{\tau_{i-1},\theta}, & \tau_i > 1, m_{\tau^{(n)}_{i-1},\theta} = 0 \\ \tau_i - \tau_{i-1}, & \tau_i > 1, m_{\tau^{(n)}_{i-1},\theta} = 1 \\ 0, & \tau_i = 1 \end{cases} \tag{1}$$

2.3 Construction of Time-Feature Fusion Model (TFF-MHA)

In our research, we have constructed an innovative model founded on the principles of multi-head self-attention (MHA). This model is uniquely designed to directly learn representations from multivariate sparse and irregularly sampled time series data, eliminating the need for imputation. At its core, the model employs a self-attention mechanism [30], where a scaled dot-product attention is computed based on a set of queries (Q), keys (K), and values (V), as delineated in the equation:

$$\alpha(Q, K, V) = \sigma\left(\frac{QK^T}{\sqrt{d_k}}\right)V \tag{2}$$

where α denotes the attention function, σ is the softmax activation function, and d_k is the dimension of the key vector. Multi-head attention allows the model to jointly attend to information from different representation subspaces at different positions.

Based on the MHA block, we learn the attention representations of multi-view irregular time series including observed values, time distance, and vacancy marker. Specifically, each input set (X, M, Δ) learns its own representation through self-attention, where each data is feed corresponding to Q, K, and V. As demonstrated in Fig. 4, the architecture of our proposed time-feature fusion multi-head attention (TFF-MHA) model is structured into three submodules. Module 1, the multi-dimensional third-order tensor data extraction, is responsible for extracting and structuring data in a tensor format, enhancing the model's ability to process complex data relationships; Module 2, the multi-head attention mechanism model, focuses on capturing intricate dependencies and relationships within the data through a sophisticated attention mechanism; and finally, Module 3, the output module, integrates the processed information from the previous modules to produce the final output, effectively consolidating and interpreting the analyzed data. To enhance our model's robustness, we also developed a basic LSTM-based neural network (standard LSTM) and introduced a variant known as channel-wise LSTM [31]. We conducted comprehensive testing and comparisons of both LSTM types against our TFF-MHA model. The TFF-MHA and LSTM models were tuned using a grid search method to find the optimal set of hyperparameters. For the TFF-MHA model, the learning rate was varied from 0.0001 to 0.01, the number of attention heads was set to 6, and the batch size was selected as 32 based on validation performance. For the LSTM model, the number of layers was varied between 2 and 4, and the dropout rate was tested from 0.2 to 0.5. Through meticulous hyperparameter search and evaluation on the test sets of corresponding tasks, we ensured the selection of the best-performing models, thereby solidifying the effectiveness and precision of our approach in dealing with complex time series data.

3 Results

3.1 Performance Comparison Across Models

Table 1 delineates the comparative efficacy of the TFF-MHA model against the standard LSTM and CM-LSTM in predicting serum sodium level abnormalities. Historically, LSTM and its variants have demonstrated commendable performance in regular time series data analysis. The TFF-MHA model, however, exhibited superior performance across various time windows (24-h, 48-h, and 72-h) in both internal testing and external validation settings. In internal testing, the TFF-MHA model achieved a sensitivity of 0.804 ($\pm$0.165), accuracy of 0.811 ($\pm$0.147), F1-score of 0.823 ($\pm$0.150), and AUC of 0.837 ($\pm$0.172). The external testing results were similarly impressive, with sensitivity, accuracy, F1-score, and AUC values of 0.813 ($\pm$0.109), 0.819 ($\pm$0.117), 0.837 ($\pm$0.121), and 0.842 ($\pm$0.106), respectively. Notably, the 48-h window data showed enhanced performance in internal validation compared to the 72-h data, further underscoring the model's robustness.

MAE mean absolute error, *RMSE* root mean square error.

The results in Table 2 focus on the prediction of serum sodium values. The TFF-MHA model outshined its counterparts across all time window comparisons.

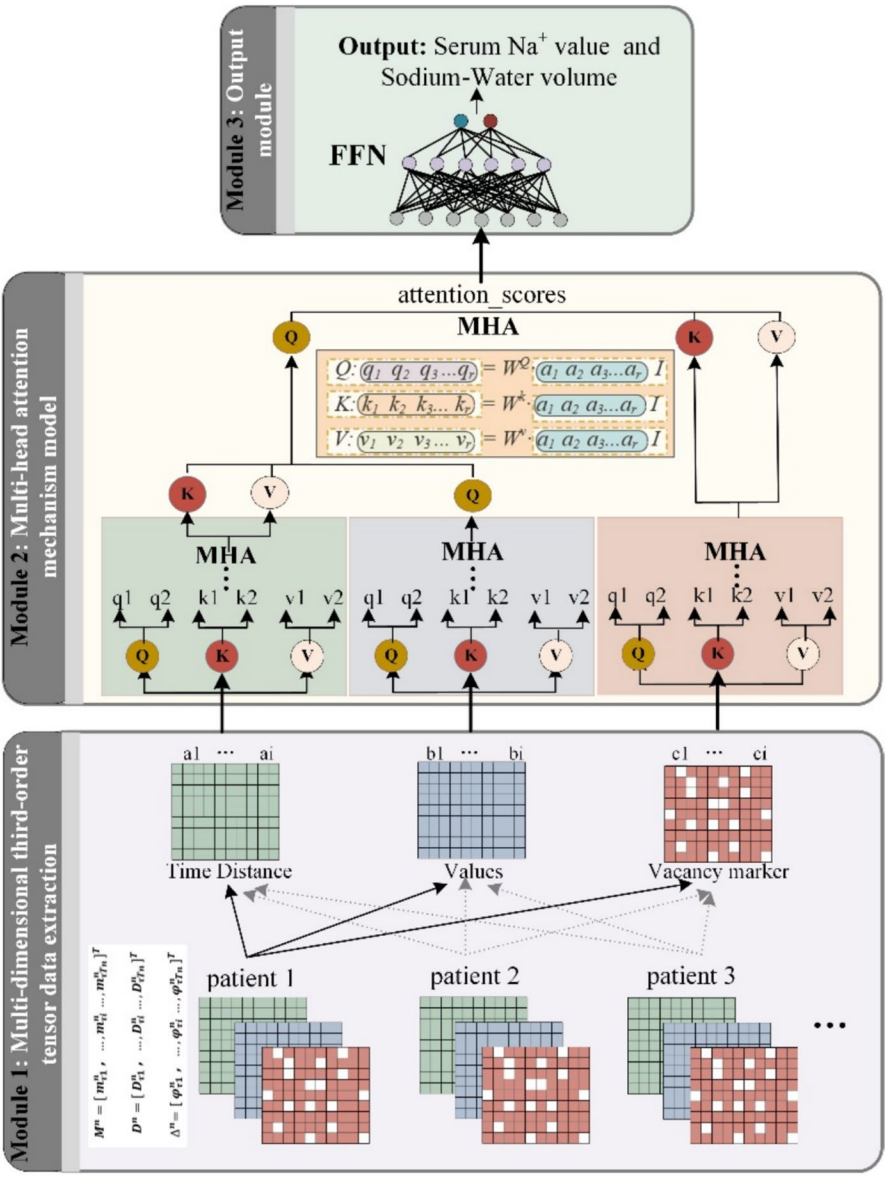

Fig. 4 The overall framework of the proposed time-feature fusion multi-head attention (TFF-MHA) model for irregularly sampled clinical time series. TFF-MHA model is structured into three submodules: Module 1, Module 2, and Module 3. The three submodules respectively handle data input, processing and modeling, and output functions.The green, yellow, and red lattice matrixes at the bottom represent the interactive information of the time, features, and missing data extracted from the irregular sampling time series. MHA is the multi-head attention module, and FFN is the fully connected neural network

Table 1 Results for prediction task of serum sodium abnormality by three methods in the internal validation and the external testing data set (all numbers represent mean ± standard deviation, the bold values in the table represent the best performance metrics predicted by the model)

	Model	Time window (hours)	Sensitivity	Specificity	F1-score	AUC-ROC
Internal validation	TFF-MHA	24	0.783 (±0.211)	0.792 (±0.197)	0.801 (±0.201)	0.809 (±0.192)
		48	**0.804 (±0.165)**	**0.811 (±0.147)**	**0.823 (±0.150)**	**0.837 (±0.172)**
		72	0.801 (±0.129)	0.794 (±0.201)	0.819 (±0.105)	0.825 (±0.124)
	S-LSTM	24	0.742 (±0.211)	0.754 (±0.190)	0.754 (±0.184)	0.762 (±0.181)
		48	0.773 (±0.117)	0.779 (±0.142)	0.763 (±0.113)	0.789 (±0.123)
		72	0.761 (±0.105)	0.765 (±0.129)	0.759 (±0.101)	0.775 (±0.116)
	CW-LSTM	24	0.762 (±0.219)	0.764 (±0.232)	0.769 (±0.185)	0.776 (±0.191)
		48	0.781 (±0.105)	0.785 (±0.127)	0.783 (±0.118)	0.798 (±0.120)
		72	0.761 (±0.105)	0.762 (±0.102)	0.784 (±0.128)	0.786 (±0.121)
External testing	TFF-MHA	24	0.791 (±0.215)	0.798 (±0.234)	0.818 (±0.211)	0.823 (±0.181)
		48	**0.813 (±0.109)**	**0.819 (±0.117)**	**0.837 (±0.121)**	**0.842 (±0.106)**
		72	0.811 (±0.110)	0.824 (±0.104)	0.831 (±0.125)	0.838 (±0.121)
	S-LSTM	24	0.739 (±0.195)	0.741 (±0.202)	0.748 (±0.213)	0.751 (±0.198)
		48	0.771 (±0.127)	0.775 (±0.136)	0.759 (±0.141)	0.791 (±0.129)
		72	0.759 (±0.104)	0.761 (±0.130)	0.769 (±0.123)	0.771 (±0.120)
	CW-LSTM	24	0.771 (±0.195)	0.783 (±0.216)	0.789 (±0.231)	0.809 (±0.222)
		48	0.791 (±0.185)	0.798 (±0.172)	0.813 (±0.171)	0.818 (±0.180)
		72	0.798 (±0.158)	0.801 (±0.162)	0.814 (±0.160)	0.815 (±0.139)

Remarkably, the 48-h window yielded the most optimal results, showcasing a correlation coefficient of 0.86(±0.09), mean absolute error of 3.64(±0.12), and root mean square error of 4.12(±0.11). In this scenario, the CW-LSTM model's performance surpassed that of the S-LSTM model, indicating its relative effectiveness in this specific task.

Table 2 Results of R^2, MAE, and RMSE by three methods in the task of serum sodium value prediction

Method	Time window (hours)	R^2	MAE	RMSE
TFF-MHA	24	0.79 (±0.08)	5.31 (±0.19)	5.94 (±0.10)
	48	0.86 (±0.09)	3.64 (±0.12)	4.12 (±0.11)
	72	0.83 (±0.11)	3.77 (±0.08)	4.39 (±0.07)
S-LSTM	24	0.71 (±0.05)	9.01 (±0.13)	9.76 (±0.15)
	48	0.79 (±0.06)	7.23 (±0.11)	7.85 (±0.16)
	72	0.77 (±0.07)	7.01 (±0.14)	7.64 (±0.13)
CW-LSTM	24	0.76 (±0.12)	7.72 (±0.07)	8.48 (±0.09)
	48	0.81 (±0.11)	6.42 (±0.09)	6.94 (±0.12)
	72	0.79 (±0.05)	6.48 (±0.08)	7.13 (±0.11)

Table 3 Results of MAE and RMSE by three methods in the task of sodium-water volume prediction

Method	Time window (hours)	MAE	RMSE
TFF-MHA	24	0.35 (±0.15)	0.41 (±0.14)
	48	0.21 (±0.15)	0.27 (±0.12)
	72	0.32 (±0.17)	0.38 (±0.11)
S-LSTM	24	0.65 (±0.19)	0.69 (±0.18)
	48	0.51 (±0.18)	0.58 (±0.20)
	72	0.57 (±0.13)	0.61 (±0.16)
CW-LSTM	24	0.45 (±0.16)	0.52 (±0.15)
	48	0.38 (±0.10)	0.44 (±0.21)
	72	0.42 (±0.21)	0.47 (±0.13)

MAE mean absolute error, *RMSE* root mean square error

Table 3 presents an evaluation of model performance in the context of sodium water regulation interventions. Here again, the TFF-MHA model demonstrated superior performance across the board, with its 48-h window data standing out. The model achieved a correlation coefficient of 0.83 (±0.12), mean absolute error of 0.21 (±0.15), and root mean square error of 0.27 (±0.12). Interestingly, the CW-LSTM model not only outperformed the S-LSTM model but also showed commendable results in the 48-h window, with a correlation coefficient of 0.80 (±0.07), mean absolute error of 0.38 (±0.10), and root mean square error of 0.44 (±0.21).

3.2 Personalized Prediction and Intervention Output Analysis

In a groundbreaking endeavor to tailor the TFF-MHA model for individual patient needs, this study meticulously selected six patients from a previously untouched subset of data across two databases. These databases had not contributed to the initial training and testing phases of the model. This selection aimed to provide a demonstrative and comparative insight into the model's predictive capabilities.

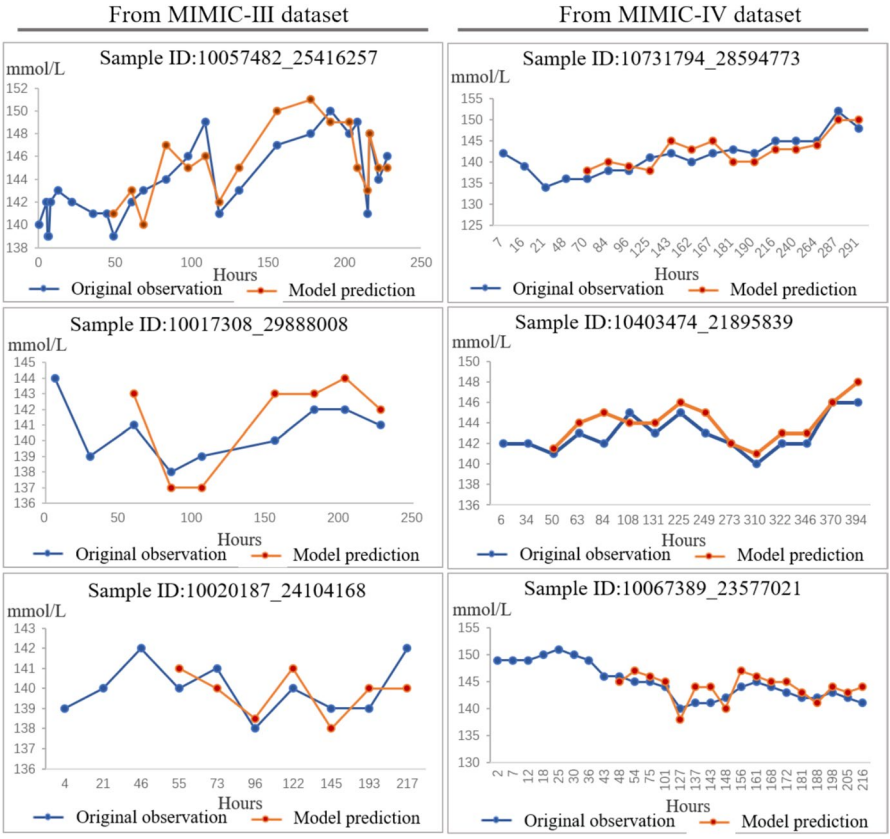

Fig. 5 Reconstructed time series of serum sodium in comparison with original observed time series. All time series of serum sodium of six patients were randomly selected from two data sets for prediction and comparison display. The blue line represents the original time series of serum sodium, and the orange line represents the splicing of blood sodium values predicted by TFF-MHA model with 48-h time window data. Therefore, the orange line did not display values in the first 48 h

Figure 5 offers a compelling visual representation of the serum sodium levels for the six chosen patients, with data randomly sourced from the two datasets. This figure distinctly marks the original serum sodium levels (blue line) against the model's continuous predictions (orange line), utilizing a 48-h time window data. Notably, the initial 48-h period remains prediction-free in the orange line, as this timeframe constitutes the minimum data segment required for model training, thereby precluding any predictive output. The close alignment of the model's predictions with the actual serum sodium values is a testament to its accuracy and precision in fitting the data.

The study extends its focus to stroke patients, particularly addressing the critical aspect of sodium fluid dosage control. Figure 6 parallels Fig. 5 in structure, showcasing the individualized predicted sodium fluid dosage for the same six patients. Here, patient IDs remain consistent across both figures for coherence. The dosage

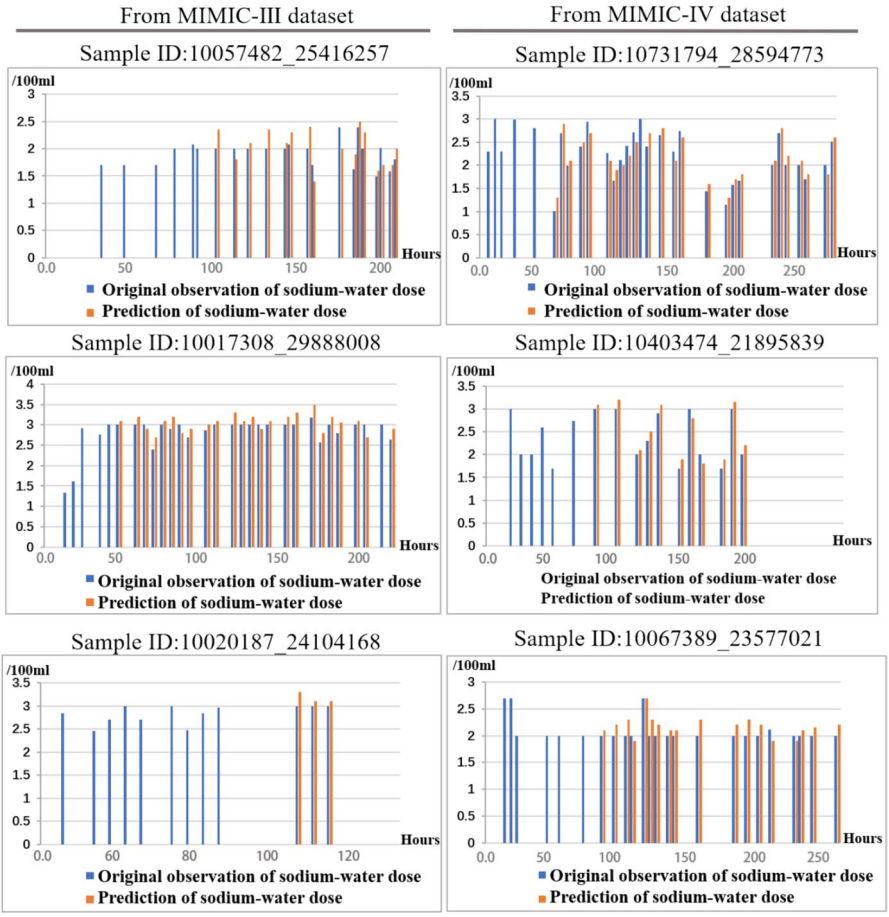

Fig. 6 Personalized prediction of sodium-water dosage. The ID of six patients randomly selected from the two data sets is consistent with that in Fig. 5. The vertical axis is the dosage of sodium water, with 100 ml as a unit, and the horizontal axis is the time point of administration after admission to the ICU. The blue line represents the actual recorded dosage, and the orange line represents the dosage predicted by the TFF-MHA model. No prediction was made in the first 48 h

amounts, represented on the vertical axis, have been normalized to 100-ml units, accommodating the vast range observed in the original data (10 to 1000 ml). This normalization process was crucial to eliminate any training biases stemming from raw value discrepancies. The horizontal axis reflects the timeline of dosage administration post-admission to the ICU. The actual recorded dosages (blue line) and the TFF-MHA model's predictions (orange line) are plotted for comparison. Similar to Fig. 5, the model commences its predictions post the 48-h mark. The striking similarity between the predicted and actual dosages highlights the model's remarkable accuracy. Clinical physicians, upon reviewing these predictive results, have affirmed their reliability and applicability in a clinical setting.

4 Discussion

The significance of predicting and intervening in serum sodium levels, particularly for stroke patients in ICU, cannot be overstated. Serum sodium imbalances, including both hypernatremia and hyponatremia, are associated with significant morbidity and mortality, underscoring the need for accurate prediction and timely intervention. People whose middle-age serum sodium exceeds 142 mmol/l have increased risk to be biologically older, develop chronic diseases, and die at younger age [32]. Research indicates that abnormalities in serum sodium, calcium, and potassium levels are significant predictors of disease progression and 30-day mortality in COVID-19 patients, highlighting the clinical importance of monitoring and managing these electrolyte levels [33]. Additionally, prior fluid and electrolyte imbalances have been associated with an increased risk of death, independent of age, and prior renal comorbidities, further emphasizing the need for early detection and management of these imbalances [34]. The advent of artificial intelligence in healthcare, particularly in the development of deep learning models using electrocardiography for detecting electrolyte imbalances, offers a promising avenue for enhancing the precision of electrolyte management in real-time clinical settings [35]. Collectively, these studies underscore the critical need for ongoing research and development in the field of serum sodium prediction and intervention, which could lead to improvements in patient outcomes, especially in high-risk populations.

Interventions for dysnatremias primarily stem from clinical experience, with many studies focusing on the optimal rate of correction of serum sodium levels. Some studies indicated that hypernatremia correction rate should not exceed 0.5 mmol/L/h or 10 mmol/L/d to avoid the development of cerebral edema and permanent neurological damage [36–38]. These complications were documented mainly in neonates [39, 40]. Several small studies reported that slow correction of hypernatremia is associated with excess mortality [41, 42]. A recent study found no association between rate of correction of hypernatremia and clinical outcomes [36]. Whether the existing guidelines strike the best balance between ensuring patient safety and minimizing possible harm remains uncertain.

In the field of medicine, the application of artificial intelligence enables the prediction and resolution of complex issues that are difficult to handle with traditional methods. The development of our TFF-MHA model marks a significant advancement in predicting serum sodium abnormalities in stroke patients. By effectively learning from sparse and irregularly sampled time series data, the model eliminates the need for traditional data imputation methods. Its ability to integrate diverse data points, including missing indicators and time intervals, not only enhances the accuracy of predictions but also provides a more comprehensive understanding of the underlying physiological processes. This holistic approach is particularly crucial in managing complex stroke cases, where timely and accurate predictions can significantly influence patient outcomes. Compared to traditional predictive methods, such as the four formulas evaluated in the study [43], the TFF-MHA model not only handles more complex datasets but also provides more accurate and individualized predictions. This is particularly crucial in managing hypernatremic and normonatremic

ICU patients, as traditional formulas have limitations in predicting individual patient's serum sodium changes. In a study anchored in the principles of mass conservation, researchers endeavored to predict sodium fluctuations in patients within ICU [44]. This research necessitated the rigorous collection of plasma and urine samples to measure sodium levels, integrating these findings with existing serum sodium prediction formulas to develop a novel mathematical model. In contrast, the time-feature fusion multi-head attention (TFF-MHA) model offers a paradigmatic shift by amalgamating time series data from various clinical indicators and temporal metrics. This holistic approach facilitates a more comprehensive understanding and prediction of electrolyte imbalances, particularly enhancing the precision of predictions in complex and acute clinical scenarios. Moreover, research focusing on severe hyponatremia underscores the importance of predictive correction of serum sodium concentrations [45]. In this context, the TFF-MHA model demonstrates unique strengths, not only in forecasting the risk of electrolyte imbalances but also in providing insights into optimal intervention strategies.

While the model exhibited better predictive performance, its generalizability across diverse healthcare settings may be influenced by variations in patient demographics and clinical practices. Further research is required to assess the model's real-time utility and effectiveness in clinical environments. Future efforts will focus on expanding the model to predict additional critical electrolytes, such as potassium and calcium, which play vital roles in stroke management. Moreover, incorporating other physiological parameters, such as body temperature and respiratory rate, holds potential to further improve the model's accuracy and enhance its clinical applicability. In the future, to integrate the model into clinical decision support systems (CDSS), it can be connected to electronic health record (EHR) systems for real-time data access, deployed either locally or on the cloud, and optimized for different clinical environments. The model's outputs can be presented through an intuitive user interface that allows clinicians to make informed decisions, with continuous feedback to refine its performance. Data privacy is ensured through encryption and anonymization, while compliance with regulations such as HIPAA and GDPR is maintained. Additionally, training and ongoing support for clinical staff will facilitate effective integration and use of the system.

In summary, the TFF-MHA model shows potential in predicting and managing electrolyte imbalances. It not only offers a more refined and comprehensive approach to analyzing and predicting electrolyte imbalances but also provides individualized intervention recommendations on a patient-specific level. This approach holds implications for improving patient outcomes and optimizing the allocation of clinical resources.

5 Conclusion

In conclusion, we established a novel deep learning model: TFF-MHA model, proficient in learning from multivariate, sparse, and irregularly sampled time series data, eliminating the need for imputation. It has shown capability in predicting both serum

sodium values and necessary interventions, thereby providing timely and critical clinical insights to prevent the adverse outcomes of delayed medical interventions.

Abbreviations AUC: Area under the curve; LSTM: Channel-wise long short-term memory; EHR : Electronic health record; FFN : Feed forward network; HTS: Hypertonic saline; ICD10: International Classification of Diseases, Tenth Revision; ICD9: International Classification of Diseases, Ninth Revision; ICP: Intracranial pressure; ICU: Intensive care unit; IMTS: Irregular multivariate time series; LSTM: Long short-term memory; MHA: Multi-head attention; MIMIC-III: Medical Information Mart for Intensive Care III; MIMIC-IV: Medical Information Mart for Intensive Care IV; STROBE: Strengthening the Reporting of Observational Studies in Epidemiology; TFF-MHA: Time-feature fusion multi-head attention

Acknowledgements We would like to express our gratitude to the Biological & Medical Engineering Core Facilities of Beijing Institute of Technology and the Big Data Center Platform of the PLA General Hospital.

Author Contributions Xiao Lu was the primary investigator, leading the study design and conducting the experiments.Hongli Xu involved in the proof reading of the paper and the modification of the model. Hebin Che, together with Xingkang Lin and Jiang Zhu., was responsible for data collection and statistical analysis. Wei Dong, Yin Xin and Zhuang Yan contributed their clinical expertise, significantly guiding the manuscript's writing process. Qin Li and Kunlun He played a crucial role in critically reviewing and refining both the study design and the manuscript. All authors have thoroughly reviewed and given their final approval for the publication of this manuscript.

Funding This work was supported by the Research Project (BHQ090003000X03), Noncommunicable Chronic Diseases-National Science and Technology Major Project (2023ZD0504703), and Beijing Natural Science Foundation (L222006).

Data Availability The original data are available in the MIMIC repository, https://physionet.org/content/mimic/. The datasets used and analyzed in the current study are available from the corresponding author upon reasonable request.

Declarations

Ethics Approval The study aligned with ethical standards, received approval from the ethics committee of the PLA General Hospital. It was conducted in adherence to the World Medical Association Declaration of Helsinki Ethical Principles for Medical Research Involving Human Subjects.

Consent for Publication All listed authors consented to the submission and all data were used with the consent of the person generating the data.

Competing Interests The authors declare no competing interests.

References

1. Eagles ME, Tso MK, Macdonald RL (2018) Significance of fluctuations in serum sodium levels following aneurysmal subarachnoid hemorrhage: an exploratory analysis. J Neurosurg 131(2):420–425
2. Wijdicks EF et al (2014) Recommendations for the management of cerebral and cerebellar infarction with swelling: a statement for healthcare professionals from the American Heart Association/ American Stroke Association. Stroke 45(4):1222–1238
3. Torbey MT et al (2015) Evidence-based guidelines for the management of large hemispheric infarction : a statement for health care professionals from the Neurocritical Care Society and the German Society for Neuro-intensive Care and Emergency Medicine. Neurocrit Care 22(1):146–164
4. Wang Z et al (2017) Age-period-cohort analysis of stroke mortality in China: Data From the Global Burden of Disease Study 2013. Stroke 48(2):271–275
5. Guan T et al (2017) Rapid transitions in the epidemiology of stroke and its risk factors in China from 2002 to 2013. Neurology 89(1):53–61
6. Fu X et al (2013) Factors associated with severity on admission and in-hospital mortality after primary intracerebral hemorrhage in China. Int J Stroke 8(2):73–79
7. Soiza RL et al (2015) Hyponatremia predicts mortality after stroke. Int J Stroke 10(100):50–5
8. Adekunle-Olarinde IR et al (2017) Addition of sodium criterion to SOAR stroke score. Acta Neurol Scand 135(5):553–559
9. Hoorn EJ, Zietse R (2013) Hyponatremia and mortality: moving beyond associations. Am J Kidney Dis 62(1):139–149
10. Chawla A et al (2011) Mortality and serum sodium: do patients die from or with hyponatremia? Clin J Am Soc Nephrol 6(5):960–965
11. Hecking M et al (2012) Predialysis serum sodium level, dialysate sodium, and mortality in maintenance hemodialysis patients: the Dialysis Outcomes and Practice Patterns Study (DOPPS). Am J Kidney Dis 59(2):238–248
12 Mc Causland FR, Brunelli SM, Waikar SS (2012) Dialysate sodium, serum sodium and mortality in maintenance hemodialysis. Nephrol Dial Transplant 27(4):1613–8
13. Barsony J, Sugimura Y, Verbalis JG (2011) Osteoclast response to low extracellular sodium and the mechanism of hyponatremia-induced bone loss. J Biol Chem 286(12):10864–10875
14. Griesdale DE, Sekhon MS, Henderson WR (2013) Hypernatremia and intracranial pressure: more questions than answers. Crit Care 17(1):401
15. Tan SK et al (2016) The effect of continuous hypertonic saline infusion and hypernatremia on mortality in patients with severe traumatic brain injury: a retrospective cohort study. Can J Anaesth 63(6):664–673
16. Janett RS, Yeracaris PP (2020) Electronic medical records in the American Health System: challenges and lessons learned. Cien Saude Colet 25(4):1293–1304
17. Callahan A, Shah NH, Chen JH (2020) Research and reporting considerations for observational studies using electronic health record data. Ann Intern Med 172(11 Suppl):S79–S84
18. Kaplan AD et al (2022) Continuous-time probabilistic models for longitudinal electronic health records. J Biomed Inform 130:104084
19. Iqbal A et al (2024) Anomaly detection in multivariate time series data using deep ensemble models. PLoS ONE 19(6):e0303890
20. Lee S et al (2024) Rapid deep learning-assisted predictive diagnostics for point-of-care testing. Nat Commun 15(1):1695
21. Sattar S et al (2024) Cardiac arrhythmia classification using advanced deep learning techniques on digitized ECG datasets. Sensors 24(8):2484
22. Heo J et al (2019) Machine learning-based model for prediction of outcomes in acute stroke. Stroke 50(5):1263–1265
23. D'Ascenzo F et al (2021) Machine learning-based prediction of adverse events following an acute coronary syndrome (PRAISE): a modelling study of pooled datasets. Lancet 397(10270):199–207
24. Tokodi M et al (2020) Machine learning-based mortality prediction of patients undergoing cardiac resynchronization therapy: the SEMMELWEIS-CRT score. Eur Heart J 41(18):1747–1756
25. Lipton ZC, Kale D, Wetzel R (2016) Directly modeling missing data in sequences with rnns: improved classification of clinical time series. In: Machine learning for healthcare conference. PMLR 253–270
26. Futoma J, Hariharan S, Heller K (2017) Learning to detect sepsis with a multitask Gaussian process RNN classifier. PMLR 1174–1182

27. Johnson A et al. (2021) MIMIC-IV (version 1.0). PhysioNet [J]. https://doi.org/10.13026/s6n6-xd98
28. Johnson AE et al (2016) MIMIC-III, a freely accessible critical care database. Scientif Data 3(1):1–9
29. von Elm E et al (2014) The Strengthening the Reporting of Observational Studies in Epidemiology (STROBE) statement: guidelines for reporting observational studies. Int J Surg 12(12):1495–1499
30. Vaswani A, et al. (2017) Attention is all you need. [J]. Advances in neural information processing systems 30
31 Harutyunyan H, Khachatrian H, Kale DC, VerSteeg G, Galstyan A (2019) Multitask learning and benchmarking with clinical time series data. Scientif Data 6(1):96
32. Dmitrieva NI et al (2023) Middle-age high normal serum sodium as a risk factor for accelerated biological aging, chronic diseases, and premature mortality. EBioMedicine 87:104404
33 Hoca NT, Berktaş BM (2022) Baseline electrolyte disorders predict disease severity and mortality in patients with COVID-19. Medicine 101(51):e32397
34. Nahkuri S et al (2021) Prior fluid and electrolyte imbalance is associated with COVID-19 mortality. Communicat Med 1(1):51
35 Kwon JM et al (2021) Artificial intelligence for detecting electrolyte imbalance using electrocardiography. Annals Noninvasive Electrocardiol 26(3):e12839
36. Chauhan K et al (2019) Rate of correction of hypernatremia and health outcomes in critically ill patients. Clinic J Am Soc Nephrol: CJASN 14(5):656
37. Muhsin SA, Mount DB (2016) Diagnosis and treatment of hypernatremia. Best Pract Res Clin Endocrinol Metab 30(2):189–203
38. Braun MM, Barstow CH, Pyzocha NJ (2015) Diagnosis and management of sodium disorders: hyponatremia and hypernatremia. Am Fam Physician 91(5):299–307
39. Bolat F et al (2013) What is the safe approach for neonatal hypernatremic dehydration?: a retrospective study from a neonatal intensive care unit. Pediatr Emerg Care 29(7):808–813
40. Kahn A, Brachet E, Blum D (1979) Controlled fall in natremia and risk of seizures in hypertonic dehydration. Intensive Care Med 5:27–31
41. Bataille S et al (2014) Undercorrection of hypernatremia is frequent and associated with mortality. BMC Nephrol 15(1):1–9
42. Alshayeb HM et al (2011) Severe hypernatremia correction ratemortality in hospitalized patients. Am J Med Sci 341(5):356–360
43. Lindner G et al (2008) Can we really predict the change in serum sodium levels? An analysis of currently proposed formulae in hypernatraemic patients. Nephrol Dial Transplant 23(11):3501–3508
44. Katsiampoura A et al (2018) Prediction of dysnatremias in critically ill patients based on the law of conservation of mass. Comparis Exist Formul Plos one 13(11):e0207603
45. Nagase K et al (2023) Predictive correction of serum sodium concentration with formulas derived from the Edelman equation in patients with severe hyponatremia. Sci Rep 13(1):1783

Authors and Affiliations

Xiao Lu[1] · Hongli Xu[1] · Wei Dong[1] · Yi Xin[2] · Jiang Zhu[2] · Xingkang Lin[2] · Yan Zhuang[1] · Hebin Che[1] · Qin Li[2] · Kunlun He[1]

✉ Qin Li
liqin@bit.edu.cn

✉ Kunlun He
kunlunhe@plagh.org

[1] Medical Innovation Research Department of PLA General Hospital, Haidian District, No.28 Fuxing Road, Beijing 100853, China

[2] Department of Biomedical Engineering, School of Life Science, Beijing Institute of Technology, Beijing 100081, China